Stochastic optical reconstruction microscopy–based relative localization analysis (STORM-RLA) for quantitative nanoscale assessment of spatial protein organization

Rengasayee Veeraraghavan[a,*] and Robert G. Gourdie[a,b,*]
[a]Center for Heart and Regenerative Medicine Research, Virginia Tech Carilion Research Institute, Roanoke, VA 24016;
[b]School of Biomedical Engineering and Sciences, Virginia Polytechnic University, Blacksburg, VA 24016

ABSTRACT **The spatial association between proteins is crucial to understanding how they function in biological systems. Colocalization analysis of fluorescence microscopy images is widely used to assess this. However, colocalization analysis performed on two-dimensional images with diffraction-limited resolution merely indicates that the proteins are within 200–300 nm of each other in the *xy*-plane and within 500–700 nm of each other along the *z*-axis. Here we demonstrate a novel three-dimensional quantitative analysis applicable to single-molecule positional data: stochastic optical reconstruction microscopy–based relative localization analysis (STORM-RLA). This method offers significant advantages: 1) STORM imaging affords 20-nm resolution in the *xy*-plane and <50 nm along the *z*-axis; 2) STORM-RLA provides a quantitative assessment of the frequency and degree of overlap between clusters of colabeled proteins; and 3) STORM-RLA also calculates the precise distances between both overlapping and nonoverlapping clusters in three dimensions. Thus STORM-RLA represents a significant advance in the high-throughput quantitative assessment of the spatial organization of proteins.**

Monitoring Editor
Kerry S. Bloom
University of North Carolina

Received: Feb 25, 2016
Revised: Jun 7, 2016
Accepted: Jun 9, 2016

INTRODUCTION

Biological studies make wide use of colocalization analysis (CLA) to assess the spatial association between proteins. Colocalization is assessed from fluorescence microscopy images by the overlapping detection of two or more antigens via corresponding fluorescent antibody labels. Briefly, the proteins are labeled with corresponding antibodies with different excitation spectra, allowing them to be visualized in different colors, and colocalization is assessed by the overlap between the different colored signals in the registered composite image (Zinchuk and Grossenbacher-Zinchuk, 2014). However, diffraction-limited imaging techniques are capable of achieving only 200- to 300-nm spatial lateral resolution and 500–700 nm in the *z*-axis (Nienhaus and Nienhaus, 2016). Thus what is assessed as colocalization using such techniques could reflect a range of possibilities, from proteins directly interacting via chemical bonds to proteins located within 300 nm of each other (Figure 1; MacDonald *et al.*, 2015). In contrast, superresolution techniques such as gated stimulated emission depletion (gSTED) and stochastic optical reconstruction microscopy (STORM) achieve 20- to 25-nm resolution along the *xy*-plane and <50 nm along the *z*-axis (Huang *et al.*, 2013; Olivier *et al.*, 2013). As imaging resolution approaches the size range of protein molecules and antibodies—5–15 nm per molecule—colocalization is no longer possible, since multiple molecules cannot occupy the same space and, by definition, cannot be colocalized (Figure 1, A and B, right). Therefore we developed STORM-based relative localization analysis (STORM-RLA) for the quantitative assessment of the spatial organization of proteins that distribute near

This article was published online ahead of print in MBoC in Press (http://www.molbiolcell.org/cgi/doi/10.1091/mbc.E16-02-0125) on June 15, 2016.

The authors declare no conflicts of interest.

*Address correspondence to: Robert G. Gourdie (gourdier@vtc.vt.edu), Rengasayee Veeraraghavan (saiv@vt.edu).

Abbreviations used: BiFC-PALM, photoactivated localization microscopy with bimolecular fluorescence complementation; CLA, colocalization analysis; Cx43, connexin43; DBSCAN, density-based spatial clustering of applications with noise; FRET, Förster resonance energy transfer; gSTED, gated stimulated emission depletion; $Na_v1.5$, cardiac voltage-gated sodium channel; OCT, optimal cutting temperature compound; sCMOS, scientific complementary metal-oxide semiconductor; SHREC, single-molecule high-resolution colocalization; STORM, stochastic optical reconstruction microscopy, STORM-RLA, stochastic optical reconstruction microscopy–based relative localization analysis.

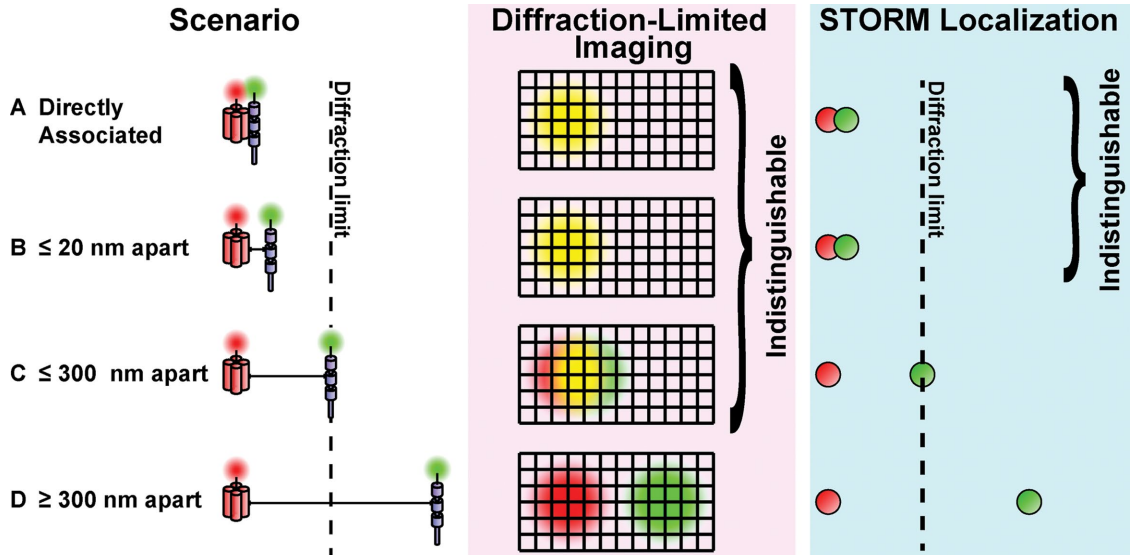

FIGURE 1: Advantages of STORM over diffraction-limited imaging techniques in assessing the spatial organization of proteins. Neither STORM nor diffraction-limited imaging can distinguish between molecules directly bound to each other (A) and those located <20 nm apart (B). However, STORM is able to distinguish the positions of molecules located >20 nm but <250–300 nm apart, whereas diffraction-limited imaging is not (C). Both techniques are able to distinguish molecules located >300 nm from each other (D). Qualitative illustration of the diffraction-limited image and STORM localizations obtained under the different scenarios.

each other with populations that partially overlap or are separated by subdiffraction distances.

Our motivation to tackle this problem and our choice of biological system for testing both stem from our ongoing research into the nanoscale structural basis of cardiac electrical excitation. Briefly, cardiac muscle cells are elongated, roughly brick-shaped cells mechanically and electrically coupled by structures termed intercalated disks (Plonsey and Barr, 2007). These intercalated disks are composed of undulating membranes with mechanical junctions located within "plicate" regions oriented perpendicular to the cell's long axis and electrical junctions (connexin43 [Cx43] gap junctions) located within "interplicate" regions oriented parallel to the cell's long axis (Kline and Mohler, 2013; Vite and Radice, 2014). Cardiac voltage-gated sodium channels ($Na_v1.5$), which play a critical role in cardiac electrical excitation, are also enriched at the intercalated disks (Petitprez *et al.*, 2011; Rhett *et al.*, 2011b, 2012). Previous results from Duolink proximity ligation assays (Rhett *et al.*, 2011b) and gSTED microscopy (Veeraraghavan *et al.*, 2015) suggested that $Na_v1.5$ was enriched near Cx43 gap junctions rather than the two proteins truly colocalizing. Therefore we viewed the Cx43-$Na_v1.5$ system in cardiac muscle as an ideal test for STORM-RLA.

RESULTS

Because intercalated disks are primarily located at the ends of the elongated cardiac muscle cells, their structure is best visualized when the cells are viewed "end on," placing the intercalated disk in en face view (i.e., oriented along the plane of the image). We obtained superresolved images of intercalated disks in en face orientation from 5-μm sections of adult guinea pig ventricular myocardium immunolabeled for Cx43 and the cardiac voltage-gated sodium channel ($Na_v1.5$). The representative STORM superresolution image in Figure 2 shows a view along the *xy*-plane of an en face intercalated disk, demonstrating close association between Cx43 in green and $Na_v1.5$ in red. Although mixed populations of Cx43 and $Na_v1.5$ could be identified in a few areas, the two proteins largely appeared to exist in closely apposed dense clusters. This is further illustrated by the close-up view (Figure 2, inset), in which a cluster of Cx43 is seen, flanked closely on either side by clusters of $Na_v1.5$. These images were generated by representing each fluorophore molecule identified by STORM as a 50-nm sphere. Note that the STORM-based localizations of molecules were obtained at 20-nm lateral resolution and 10-nm precision. The 50-nm representation was chosen merely to aid reproduction. For comparison, the region represented in Figure 2 inset is depicted in three-dimensional (3D) view in Figure 3A, with each molecule now represented as a 20-nm sphere and the volume rotated so as to better illustrate the separation between the molecules along the *z*-axis. Conversion of such positional data into an image without loss of resolution is a nontrivial computational problem. For example, a $10 \times 10 \times 10$–μm volume digitized with 8-bit precision with a voxel size of 125 nm (half the ~250-nm resolution of diffraction-limited microscopy) would generate a 0.5-MB file. The same volume digitized with 8-bit precision with a voxel size of 10 nm (half the ~20-nm resolution of STORM) would generate a 1-GB file. Manipulation of the latter image would require significant computational resources. Further, as discussed earlier, the resolution of STORM is close enough to the size of an antibody-labeled protein as to make the exact superposition of colabeled protein molecules nearly impossible. These problems limit the utility of CLA for the quantitative analysis of STORM data.

Therefore we developed STORM-RLA, which uses 3D spatial density–based cluster detection performed directly on the localized positions of molecules from STORM. The convex hulls fitted to these clusters (Figure 3B) demonstrate the fidelity of the cluster detection and hull-fitting processes. In addition, the volumes of overlap between the Cx43 and $Na_v1.5$ clusters are highlighted in yellow in Figure 3B. Of note, only small fractions of the cluster volumes were contained within the overlapping regions. The convex hulls fitted to the data from Figure 2 are shown in Figure 4. This representation enables rapid assessment of the relative spatial organization between clusters of the two labeled proteins. Further, this method also significantly lowers the computational load, since subsequent STORM-RLA calculations need only be performed on the few

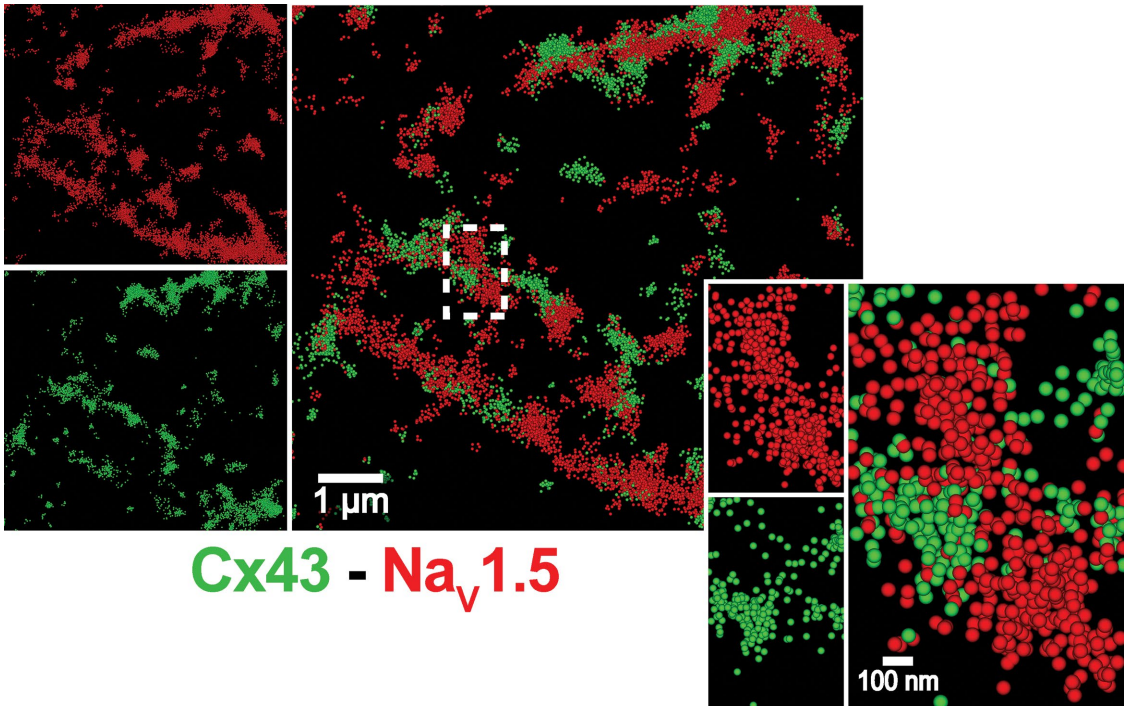

FIGURE 2: Representative STORM image showing *xy*-plane view of an en face intercalated disk. Inset, zoomed-in view of region highlighted by the dashed white box. A cluster of Cx43 is flanked on either side by clusters of $Na_v1.5$. Individual fluorophore molecules corresponding to Cx43 in green and $Na_v1.5$ in red are depicted as 50-nm spheres to generate the image (to enhance figure reproduction in print). STORM localizations were obtained at 20-nm lateral resolution.

thousand convex hull vertices for a given volume rather than on hundreds of thousands of molecules localized within it.

STORM-RLA calculates two major parameters from the convex hulls fitted to clusters of molecules. The first is the closest distances between heterotypic protein clusters. Histograms of closest intercluster distances compiled from all of the data volumes analyzed (containing a total of 623 Cx43 clusters and 1116 $Na_v1.5$ clusters) are presented in Figure 5. The distance from Cx43 clusters to their nearest $Na_v1.5$ cluster neighbors had a median value of 71 ± 33 nm, suggesting enrichment of $Na_v1.5$ close to Cx43. From the converse perspective, the median distance from $Na_v1.5$ to the nearest Cx43 cluster neighbors had a median value of 288 ± 33 nm. Taken together, these data suggest that some $Na_v1.5$ may be located in close proximity to Cx43 aggregates, whereas another significant population may be located further from Cx43. Positive intercluster distances reflect nonoverlapping clusters, represented schematically in Figure 6A (left) and by the open bars in Figure 6B. Negative intercluster distances, on the other hand, reflect clusters with some degree of overlap with their heterotypic neighbor (Figure 6B, red/green bars). However, this overlap may vary from tangential, involving very little of the volumes of the participating clusters (Figure 6A, center), all the way to total overlap, indicating a fully mixed population containing both proteins (Figure 6A, right). To distinguish between these situations, we calculated the degree of overlap, that is, the fraction of each participating cluster's volume within regions of overlap between heterotypic cluster neighbors (Figure 6C). Where overlap occurred between Cx43 and $Na_v1.5$ clusters, 32 ± 2% of the former's volume and 13 ± 4% of the latter's volume were involved in the overlap. Taken together, these data suggest that a small degree of overlap occurs between Cx43 and $Na_v1.5$ clusters; however, $Na_v1.5$ was preferentially enriched adjacent Cx43. These results are highly consistent with our previous results obtained using gSTED superresolution microscopy (Veeraraghavan *et al.*, 2015).

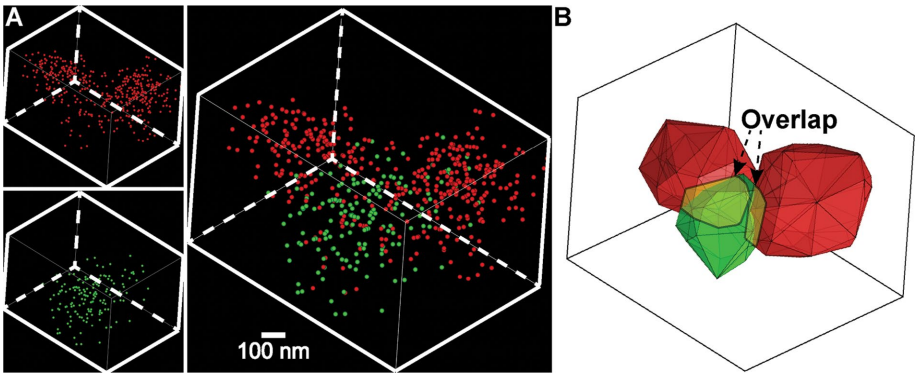

FIGURE 3: Three-dimensional rendered views of the region from the inset in Figure 2 rotated so as to illustrate the positions of the $Na_v1.5$ clusters relative to the Cx43 cluster. Left, STORM-localized molecules displayed as 20-nm spheres. Right, convex hulls fitted to the points, with the overlap between clusters highlighted in pale yellow.

DISCUSSION

The spatial organization of proteins is of vital importance to understanding the way in which proteins function within biological

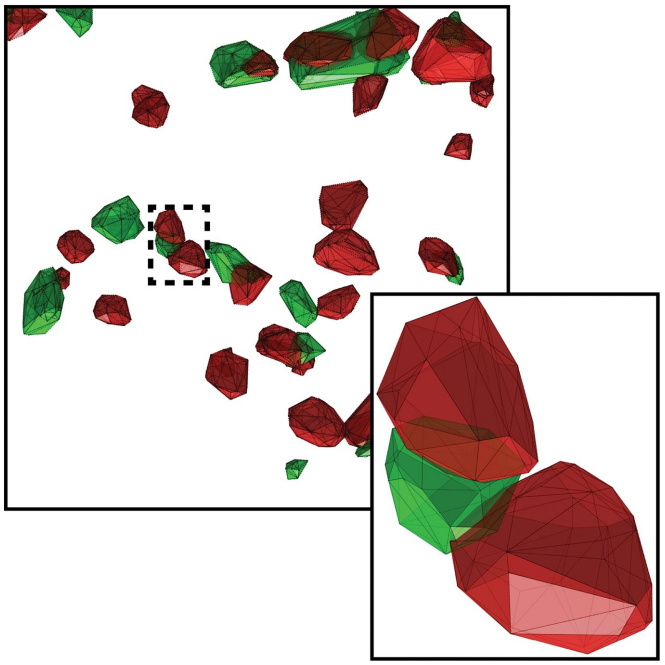

FIGURE 4: An *xy*-plane view of 3D convex hulls fitted to clusters of fluorophore molecules corresponding to Cx43 (green) and $Na_V1.5$ (red) from the image depicted in Figure 2. Inset, close-up view of the region highlighted by the dashed black box (the same region is depicted in Figure 3): a green Cx43 cluster is seen flanked on either side by red $Na_V1.5$ clusters, with some overlap occurring between clusters.

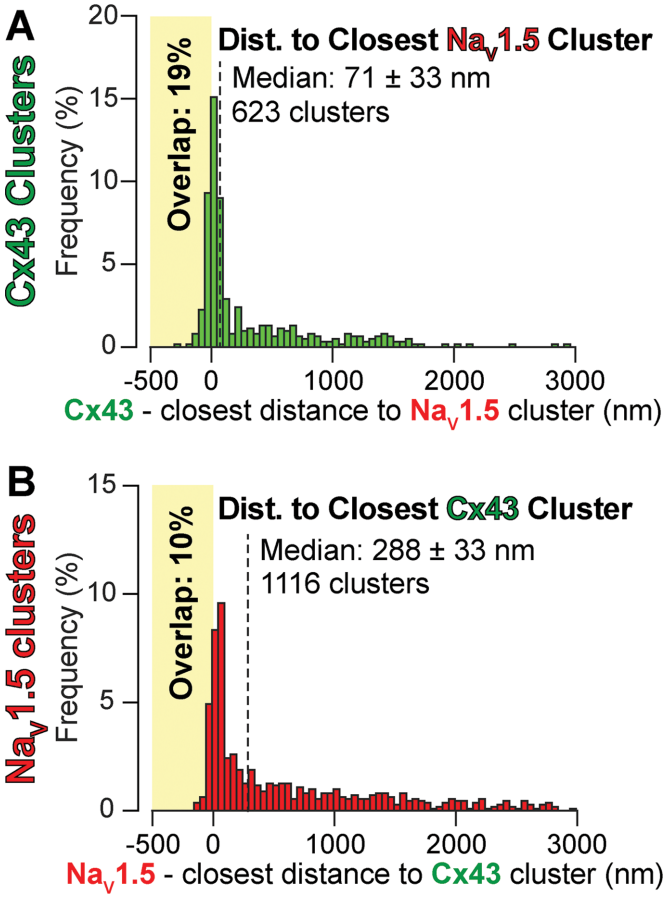

FIGURE 5: Summary histograms of closest intercluster distances between clusters of Cx43 and $Na_V1.5$ assessed by STORM-RLA. (A) Distances from all Cx43 clusters observed to their nearest $Na_V1.5$ neighbors. (B) Distances from all $Na_V1.5$ clusters observed to their nearest Cx43 neighbors. The yellow boxes on each plot highlight negative intercluster distances, which correspond to overlapping clusters. Dashed black lines mark the median values. Because Cx43 and $Na_V1.5$ are not expressed in equal quantity and do not form similar numbers of clusters, the histograms are not equivalent, that is, both histograms are necessary in order to obtain a full assessment of their relative localization.

systems, particularly given the growing appreciation of the roles of macromolecular complexes and nanodomains. Historically, most approaches to assessing the spatial organization of proteins have focused on colocalization. With resolutions approaching the size of the antibody-labeled protein molecules (20–30 nm), it becomes difficult to apply CLA to superresolution imaging techniques. Multiple molecules (proteins and antibodies) cannot occupy the same region of space; therefore, at high enough resolution, they cannot, by definition, be colocalized. Furthermore, the example of Cx43 and $Na_V1.5$ illustrates a situation in which relatively homogeneous populations of two proteins exist in close proximity to one another, separated by subdiffraction distances. Thus the need exists for methods to assess quantitatively the spatial organization of closely apposed but noncolocalizing proteins at high resolution. We describe here a novel method for quantifying relative localization of coimmunolabeled proteins from single-molecule positional data obtained using superresolution STORM imaging.

We apply this method to the analysis of STORM images of guinea pig ventricular myocardium and demonstrate that within the intercalated disk, there exists a significant subpopulation of the cardiac sodium channel, $Na_V1.5$, localized in close apposition to the gap junction protein Cx43. STORM-RLA revealed that the distance from Cx43 clusters to the nearest $Na_V1.5$ cluster neighbor was only 71 nm, suggesting that more than half of the Cx43 clusters identified had $Na_V1.5$ cluster(s) located <100 nm away. Of interest, despite the close association between the two proteins, <20% of Cx43 clusters and only 10% of $Na_V1.5$ clusters directly overlapped each other. Further, where overlap occurred, it involved less than one-third of the Cx43 cluster volume and <15% of the $Na_V1.5$ cluster volume, suggesting that the clusters overlapped tangentially rather than representing a fully mixed population of the two proteins. These findings are highly consistent with our previous results obtained using gSTED superresolution microscopy (Veeraraghavan *et al.*, 2015), providing validation of the analysis presented here. Of importance, these results identify a significant population of intercalated, disk-localized sodium channels within regions corresponding to the perinexus, a Cx43 gap junction–adjacent nanodomain (Rhett *et al.*, 2011a,b). Within the perinexus, the membranes of adjacent myocytes are apposed closely enough (5–10 nm apart) to enable these sodium channels to potentially function in electrically coupling cardiac myocytes via a noncanonical mechanism (Veeraraghavan *et al.*, 2015). This example illustrates the utility of STORM-RLA to biological research.

Historically, the spatial organization of proteins has been probed through biochemical techniques such as immunoprecipitation or imaging-based approaches such as Förster resonance energy transfer (FRET) and CLA of immunofluorescence images. However, these methods come with significant limitations. Immunoprecipitation is a complex biochemical assay and demands considerable skill in order to avoid pitfalls such as artifactual protein aggregation

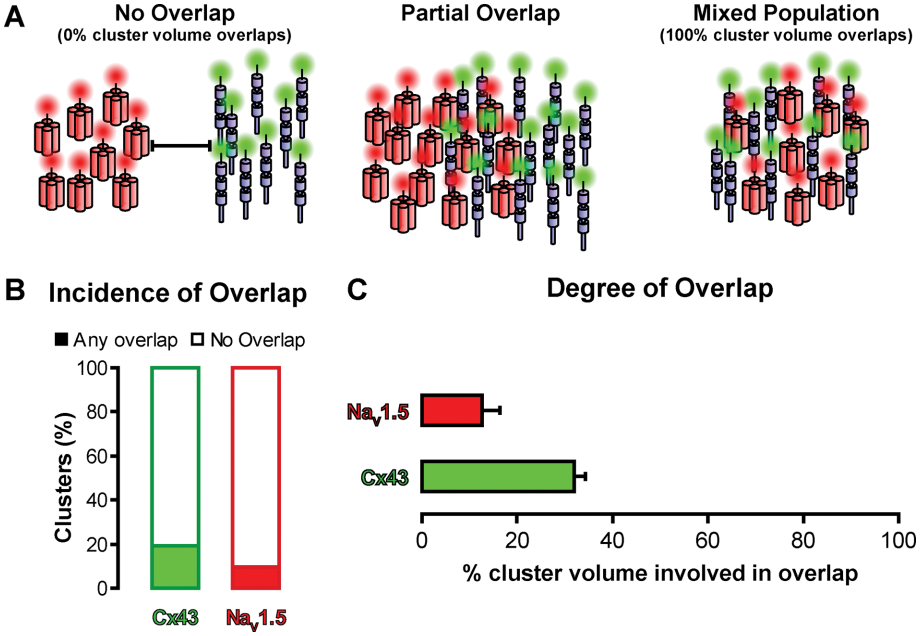

FIGURE 6: Analysis of intercluster overlap. (A) Three different scenarios corresponding to different degrees of overlap between clusters. Left, 0% overlap reflects independent populations of proteins. Center, intermediate values reflect clusters exhibiting partial overlap, ranging from tangential contact at very low values to more significant overlap at higher values. Right, 100% overlap reflects a fully mixed population of the two proteins. (B) Summary bar graph of the incidence of overlap among clusters observed. The filled bars reflect clusters demonstrating any degree of overlap, and the unfilled bars reflect nonoverlapping clusters. (C) Summary bar graph of the degree of overlap showing the fraction of cluster volume involved in overlap for those clusters that demonstrated any overlap, that is, clusters corresponding to the filled bars in B. The two ends of the *x*-axis in C correspond to the leftmost and rightmost cases illustrated in A, and midranges correspond to the middle case from A.

(Thompson, 2004; Kaboord and Perr, 2008). In addition, the technique is limited to probing proteins bonded together either directly or through interacting partners and does not reveal the spatial distribution of these interactions in relation to cellular structures. FRET is able to detect interactions only over distances of 5–10 nm (Weibrecht *et al.*, 2010), is susceptible to photobleaching, offers limited throughput, and is particularly challenging to implement in tissue, limiting its utility. Although immunofluorescence-based CLA offers both spatial information and high throughput, its resolution is limited by diffraction, that is, CLA cannot distinguish between proteins interacting directly and those located within 200–300 nm of one another (Figure 1). An important advance in this area has been the development of in situ proximity ligation assays (Weibrecht *et al.*, 2010). Briefly, the two proteins of interest are labeled with primary antibodies, followed by oligonucleotide-tagged secondary antibodies. When close enough, the oligonucleotides can be enzymatically hybridized and amplified via rolling circle amplification. These techniques offer exquisite sensitivity in detecting even infrequent interactions and are able to detect proteins within 40 nm of each other (Gullberg and Andersson, 2010); however, they offer no information on proteins located any further from each other. Further, the diffraction-limited nature of visualizing the large spot of light created by the amplification process limits the ability to correlate the observed interactions with cellular ultrastructure.

Thus superresolution imaging techniques have emerged as important tools in understanding the biology of proteins. Approaches such as photoactivated localization microscopy with bimolecular fluorescence complementation allow direct tracking of single-molecule protein–protein interactions in subdiffraction cellular space in live cells (Liu *et al.*, 2014) but are limited to probing interactions occurring over a few nanometers and cannot be easily applied to intact tissue. Recently, Delmar and coworkers demonstrated an elegant solution to the problem by correlating superresolution STORM imaging with electron microscopy (Leo-Macias *et al.*, 2016); however, this technique is highly challenging and offers very low throughput. Single-molecule high-resolution colocalization (SHREC) represents an alternative for the precise estimation of distances below the diffraction limit: briefly, the different color channels are precisely registered with each other, allowing localizations to be mapped into pixels within the image area, intensity peaks to be identified, and distances between peaks in different color channels to be calculated by Gaussian fitting of the peaks (Churchman and Spudich, 2013). STORM-RLA adapts this concept to operate in continuous 3D space by looking at clusters of localized molecules identified based on spatial density. Thus STORM-RLA enables high-throughput assessment of spatial organization of proteins, whether they exist in mixed or unmixed populations, with subdiffraction resolution and provides cell biologists with a powerful visualization tool.

STORM-RLA has further important advantages. It can be extended to any number of colabeled proteins within a sample through pairwise analysis of labeled proteins. In addition, its analytical approach can be adapted to conventional image data in two or three dimensions: Briefly, the color channels of the image corresponding to the different proteins can be converted into binary images and then subjected to cluster detection via connected component labeling based on pixel/voxel connectivity. By treating the edge pixels (two dimensions) or surface voxels (three dimensions) in the same way as convex hull vertices in STORM-RLA, intercluster distance and overlap can be quantified. A modified STORM-RLA algorithm detailing this approach is included in *Materials and Methods* (Algorithm 4).

Potential pitfalls and limitations

An important consideration when applying STORM-RLA, particularly at subdiffraction resolutions, is the registration of localized positions between color channels. Differences arise between color channels due to drift and chromatic aberrations and variations between the optical components used when the color channels are acquired via different light paths. We used an approach similar to that used in SHREC to ensure registry of localized positions between color channels: localized positions of several Tetraspeck fluorescent microspheres (ThermoFisher Scientific, Carlsbad, CA) scattered throughout the field of view were assessed and a transform calculated to register the color channels. Regardless of the imaging modality used, it is vital to ensure registry between different color channels before applying STORM-RLA analysis to the data. The potential exists for further computational optimization of STORM-RLA to speed up the

analysis. For example, the shortest intercluster distance calculation is performed using a brute-force approach by which distances are calculated between every vertex of every cluster of one protein to every vertex of every cluster of the other. This step could be optimized to minimize computational load. Further, the program was implemented in MATLAB, which is a scientific computing tool with myriad numerical analysis and visualization functions built in. Implementation using a programming language such as C++ by which algorithms would be directly implemented in the machine code of the host CPU could yield significant savings in computation time (Andrews, 2012).

Future directions

The analyses described here could potentially be expanded to make comparisons between data obtained at different time points from living preparations: This would permit the direct characterization of dynamic changes in relative protein localization by cellular processes, providing insight into the movements and interactions of the components of biological nanomachines.

Conclusion

In summary, we demonstrate here STORM-RLA, a method for the high-throughput quantitative assessment of spatial organization of proteins in subdiffraction space. Further, this method can be extended to cases in which more than two proteins are simultaneously labeled, as well as extended to conventional image data in two or three dimensions.

MATERIALS AND METHODS

The investigation was conducted in conformation with the *Guide for the Care and Use of Laboratory Animals* (Institute for Laboratory Animal Research, Commission on Life Sciences, Division on Earth and Life Studies, National Research Council, 1996). All animal study protocols were approved by the Institutional Animal Care and Use Committee at Virginia Polytechnic University.

Immunolabeling and STORM

Adult male guinea pigs (800–1000 g; $n = 3$) were anesthetized and their ventricles isolated as previously described (Veeraraghavan and Poelzing, 2008; Veeraraghavan *et al.*, 2012, 2013). Tissue blocks cut from these ventricles were embedded in OCT and frozen for cryosectioning. Sections (5 μm) were cut from frozen tissue blocks, fixed in 2% paraformaldehyde at room temperature for 5 min, and immunolabeled as previously described (Veeraraghavan *et al.*, 2015) with mouse anti-Cx43 (MAB3067, 1:100; Millipore, Billerica, CA) and rabbit anti-$Na_v1.5$ (1:100; kindly provided by Peter Mohler, SBS-Physiology & Cell Biology, The Ohio State University). Samples were then labeled with goat anti-rabbit Alexa 647 (1:4000) and donkey anti-mouse Cy3b (1:100) secondary antibodies. STORM images were obtained using a Vutara 350 microscope equipped with biplane 3D detection (Juette *et al.*, 2008; Mlodzianoski *et al.*, 2009; Deschout *et al.*, 2014) and fast scientific complementary metal-oxide-semiconductor imaging, achieving 20-nm *xy*- and 50-nm *z*-resolution. Volumes imaged had a surface extent of 10×10 to 15×15 μm and spanned between 3 and 5 μm in the *z*-dimension. Localization of particles was accomplished with a precision of 10 nm. Registration of the two color channels was achieved using a transform calculated from the localized positions of several TetraSpeck Fluorescent Microspheres (ThermoFisher Scientific, Carlsbad, CA) scattered throughout the field of view, similar to a previously described approach (Churchman and Spudich, 2013).

STORM-based relative localization analysis

Data from STORM consisted of the precise location in three dimensions of each fluorophore molecule identified. These data were analyzed using custom Matlab software (MathWorks, Natick, MA) as outlined later (Algorithm 1, Figure 7). Briefly, a modified implementation of the DBSCAN algorithm (Ester *et al.*, 1996; Algorithm 2) was used to identify clusters of molecules based on spatial density of molecules of the same fluorophore. Next a convex hull was fitted to each identified cluster using the *quickhull* algorithm (Barber *et al.*, 1996). Once this process was completed for all clusters of each fluorophore, each cluster was examined for overlap with a cluster of the other fluorophore and the degree of overlap determined (Algorithm 3). The distance from the surface of each cluster of one fluorophore to the closest point on the surface of a cluster of the other fluorophore was calculated. Note that all calculations for STORM-RLA were performed directly on the localized positions obtained from STORM, that is, in continuous space, without the data being binned into voxels. Finally, the closest intercluster distances were combined into histograms. Of note, two histograms are generated: one showing the closest distance to a protein 2 cluster from each protein 1 cluster, and the other showing the closest distance to a protein 1 cluster from each protein 2 cluster. Because different proteins are distributed differently in space, different numbers of clusters are identified for the two proteins; therefore these two histograms do not present the same information. For example, protein A may always occur near protein B; however, the converse is not necessarily true. Thus it is important to present both histograms. The following algorithms were used for these analyses.

Algorithm 1: STORM-RLA

1. Read in STORM data containing 3D positions of molecules (Figure 7-1).

2. Sort molecules into sets A and B corresponding to the two proteins labeled.

3. Perform cluster detection and convex hull fitting on A and B (Figure 7-2).

3.1. Perform cluster detection on A and B using modified DBSCAN algorithm (as detailed later).

3.2. Fit a convex hull to the points contained within the each cluster. Obtain the hull vertices for each cluster (Figure 7-3).

4. Calculate the shortest surface-to-surface distance from each cluster of proteins 1 and 2 to each cluster of the other protein (Figure 7-5) and assess whether any overlap occurs between them (Figure 7-4; as detailed later).

5. For each cluster of protein 1 or 2, identify the nearest cluster of the other protein, the distance to it, and whether any overlap occurs.

5.1. Where overlap occurs, calculate the fractions of the participating clusters located within the overlapping region.

5.2. Compile histograms of the closest intercluster distances.

Algorithm 2: modified DBSCAN algorithm

1. Load data set D containing *N* molecules.

2. Obtain neighborhood radius *NR* and minimum number of neighbors *NP*.

3. Set molecule counter $n = 1$. (Start with the first molecule in the data set.) Set cluster counter $C = 0$. (Start with no clusters.)

4. Is $n \leq N$? (Check whether data set has been exhausted.)

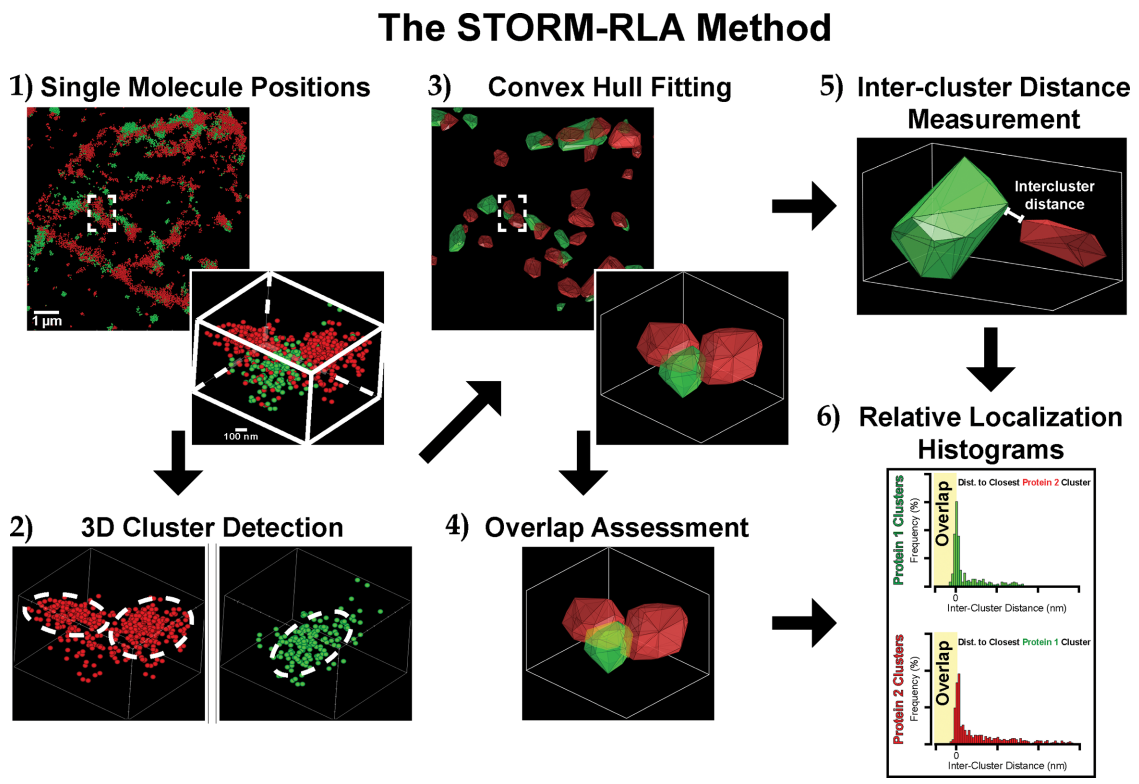

FIGURE 7: A graphical representation of the major steps involved in STORM-RLA. 1) Single-molecule positions are obtained using STORM. 2) Clusters are detected based on spatial density of molecules of the like fluorophore. 3) Convex hulls are fitted to clusters. 4) Overlap between clusters of colabeled proteins is assessed. 5) The closest surface-to-surface distance from each cluster to a cluster of the colabeled protein is calculated. 6) Closest intercluster distances are compiled into histograms. STORM-localized molecules are represented as 50-nm spheres in steps 1 and 2 in order to allow effective reproduction of the figure at small sizes.

4.1. If yes, set D(*n*) as the current molecule.

4.2. If no, skip to step 9 (end).

5. Has this molecule D(*n*) already been analyzed?

5.1. If yes, set $n = n + 1$ (skip to next molecule) and return to step 4.

5.2. If no, mark D(*n*) as analyzed.

6. Does the molecule D(*n*) have ≥*NP* molecules located ≤*NR* nanometers away?

6.1. If yes, set $C = C + 1$ (initiate a new cluster) and add D(*n*) to it.

6.2. If no, mark D(*n*) as a noncluster molecule, set $n = n + 1$ (skip to next molecule), and return to step 4.

7. Compile NL, the list of neighbors of D(*n*). Set neighbor counter, $kn = 1$.

8. Is *kn* ≤ the number of molecules currently in NL?

8.1. If no, set $n = n + 1$ (neighbors list exhausted; proceed to next molecule) and return to step 4.

8.2. If yes, set NL(*kn*) as the current neighbor point.

8.2.1. Has this molecule NL(*kn*) already been analyzed?

8.2.1.1. If yes, set $kn = kn + 1$ (skip to next neighbor molecule) and return to step 8.

8.2.1.2. If no, mark NL(*kn*) as analyzed.

8.2.2. Does the molecule NL(*kn*) have ≥*NP* molecules located ≤*NR* nanometers away?

8.2.2.1. If yes, add NL(*kn*) to the current cluster *C*.

8.2.2.2. If no, mark NL(*kn*) as a noncluster molecule, set $kn = kn + 1$ (skip to next neighbor molecule), and return to step 8.

8.2.3. Append the neighbors of NL(*kn*) to NL without duplication, set $kn = kn + 1$ (proceed to next neighbor molecule), and return to step 8.

9. End.

Algorithm 3: shortest intercluster distance and overlap calculation

1. Load hull vertices HVA and HVB for clusters of two proteins, A and B.

2. Count the number of clusters *nc*A and *nc*B contained in the respective data sets for proteins A and B.

3. Parse through the *nc*A clusters of protein A using a counter *kc*A.

3.1. Parse through *nc*B clusters of protein B using a counter *kc*B.

3.2. Assess overlap between the *kc*Ath cluster of A and the *kc*Bth cluster of B:

3.2.1. Identify any of the hull vertices from HVA(*kc*A) that are located within the hull HVB(*k*VB).

3.2.2. Identify any of the hull vertices from HVB(*kc*B) that are located within the hull HVA(*k*VA).

3.2.3. If any such vertices are identified in step 3.2.1 or 3.2.2, the two clusters overlap.

3.2.4. Fit a convex hull to the set of all vertices identified in steps 3.2.1 and 3.2.2 to estimate the volume of the overlapping region.

3.3. Calculate the shortest surface-to-surface distance between the *k*cAth cluster of A and the *k*cBth cluster of B:

3.3.1. Calculate the distance from each point in HVA(*k*cA) to each point in HVB(*k*vB).

3.3.2. Calculate the minimum distance from step 3.3.1. Multiply it by −1 if overlap was identified in step 3.2.3.

3.3.3. Set the distance between the *k*cAth cluster of A and the *k*cBth cluster of B to the value from 3.3.2.

Algorithm 4: modified STORM-RLA for image data

1. Read in image data.

2. Separate individual color channels and apply thresholds to convert each into a binary image.

3. Detect clusters in binary images using connected components labeling based on pixel/voxel connectivity.

4. Erode clusters with a 1 pixel/voxel–sized structure element and subtract the eroded image from the binary image to obtain an image of the cluster surfaces.

5. Assess overlap between clusters of proteins 1 and 2:

5.1. Check the surface pixels/voxels of each cluster of protein 1 for membership in a cluster of protein 2 and vice versa: if such membership occurs, it indicates overlap between clusters.

5.2. For each pair of overlapping clusters, identify pixels/voxels that are members of both clusters in order to determine the degree of overlap.

6. Calculate the shortest surface-to-surface distance from each cluster of proteins 1 and 2 to each cluster of the other protein and assess if any overlap occurs between them:

6.1. For each cluster of protein 1 or 2, calculate the distance from its surface pixels/voxels to the surface pixels/voxels of all clusters of the other protein.

6.2. Determine the minimum value from those calculated in step 6.1.

6.3. Compile histograms of the closest intercluster distances.

An implementation of STORM-RLA in Matlab can be downloaded from the Matlab Central File Exchange: www.mathworks.com/matlabcentral/fileexchange/57647-storm-based-relative-localization-analysis.

REFERENCES

Andrews T (2012). Computation time comparison between Matlab and C++ using launch windows. Available at http://digitalcommons.calpoly.edu/aerosp/78/.

Barber CB, Dobkin DP, Huhdanpaa H (1996). The quickhull algorithm for convex hulls. ACM Trans Math Softw (TOMS) 22, 469–483.

Churchman LS, Spudich JA (2013). Single-molecule high-resolution colocalization (SHREC). In: Encyclopedia of Biophysics, ed. GCK Roberts, Berlin: Springer, 2336–2337.

Deschout H, Cella Zanacchi F, Mlodzianoski M, Diaspro A, Bewersdorf J, Hess ST, Braeckmans K (2014). Precisely and accurately localizing single emitters in fluorescence microscopy. Nat Methods 11, 253–266.

Ester M, Kriegel H-P, Sander J, Xu X (1996). A density-based algorithm for discovering clusters in large spatial databases with noise. In: Proceedings of 2nd International Conference on Knowledge Discovery and Data Mining (KDD-96), Palo Alto, CA: Association for the Advancement of Artificial Intelligence, 226–231.

Gullberg M, Andersson A-C (2010). Visualization and quantification of protein-protein interactions in cells and tissues. Nat Methods 7, doi:10.1038/nmeth.f.306.

Huang F, Hartwich TM, Rivera-Molina FE, Lin Y, Duim WC, Long JJ, Uchil PD, Myers JR, Baird MA, Mothes W, *et al.* (2013). Video-rate nanoscopy using sCMOS camera-specific single-molecule localization algorithms. Nat Methods 10, 653–658.

Institute for Laboratory Animal Research, Commission on Life Sciences, Division on Earth and Life Studies, National Research Council (1996). Guide for the Care and Use of Laboratory Animals, Washington, DC: National Academies Press.

Juette MF, Gould TJ, Lessard MD, Mlodzianoski MJ, Nagpure BS, Bennett BT, Hess ST, Bewersdorf J (2008). Three-dimensional sub-100 nm resolution fluorescence microscopy of thick samples. Nat Methods 5, 527–529.

Kaboord B, Perr M (2008). Isolation of proteins and protein complexes by immunoprecipitation. Methods Mol Biol 424, 349–364.

Kline CF, Mohler PJ (2013). Evolving form to fit function: cardiomyocyte intercalated disc and transverse-tubule membranes. Curr Top Membr 72, 121–158.

Leo-Macias A, Agullo-Pascual E, Sanchez-Alonso JL, Keegan S, Lin X, Arcos T, Feng Xia L, Korchev YE, Gorelik J, Fenyo D, *et al.* (2016). Nanoscale visualization of functional adhesion/excitability nodes at the intercalated disc. Nat Commun 7, 10342.

Liu Z, Xing D, Su QP, Zhu Y, Zhang J, Kong X, Xue B, Wang S, Sun H, Tao Y, *et al.* (2014). Super-resolution imaging and tracking of protein-protein interactions in sub-diffraction cellular space. Nat Commun 5, 4443.

MacDonald L, Baldini G, Storrie B (2015). Does super-resolution fluorescence microscopy obsolete previous microscopic approaches to protein co-localization? Methods Mol Biol 1270, 255–275.

Mlodzianoski MJ, Juette MF, Beane GL, Bewersdorf J (2009). Experimental characterization of 3D localization techniques for particle-tracking and super-resolution microscopy. Opt Express 17, 8264–8277.

Nienhaus K, Nienhaus GU (2016). Where do we stand with super-resolution optical microscopy? J Mol Biol 428, 2 Pt A308–322.

Olivier N, Keller D, Gonczy P, Manley S (2013). Resolution doubling in 3D-STORM imaging through improved buffers. PLoS One 8, e69004.

Petitprez S, Zmoos AF, Ogrodnik J, Balse E, Raad N, El-Haou S, Albesa M, Bittihn P, Luther S, Lehnart SE, *et al.* (2011). SAP97 and dystrophin macromolecular complexes determine two pools of cardiac sodium channels Nav1.5 in cardiomyocytes. Circ Res 108, 294–304.

Plonsey R, Barr RC (2007). Bioelectricity: A Quantitative Approach, New York: Springer.

Rhett JM, Jourdan J, Gourdie RG (2011a). Connexin 43 connexon to gap junction transition is regulated by zonula occludens-1. Mol Biol Cell 22, 1516–1528.

Rhett JM, Ongstad EL, Jourdan J, Gourdie RG (2012). Cx43 associates with Na(v)1.5 in the cardiomyocyte perinexus. J Membr Biol 245, 411–422.

Rhett JM, Palatinus JA, Jourdan JA, Gourdie RG (2011b). Connexin43 interacts with voltage-gated sodium channel 1.5 in the perinexus. Circulation 124, A9561.

Thompson S (2004). Immunoprecipitation and blotting. Mol Diagn Infect Dis 33–45.

Veeraraghavan R, Larsen AP, Torres NS, Grunnet M, Poelzing S (2013). Potassium channel activators differentially modulate the effect of sodium channel blockade on cardiac conduction. Acta Physiol (Oxf) 207, 280–289.

Veeraraghavan R, Lin J, Hoeker GS, Keener JP, Gourdie RG, Poelzing S (2015). Sodium channels in the Cx43 gap junction perinexus may constitute a cardiac ephapse: an experimental and modeling study. Pflugers Arch 467, 2093–2105.

Veeraraghavan R, Poelzing S (2008). Mechanisms underlying increased right ventricular conduction sensitivity to flecainide challenge. Cardiovasc Res 77, 749–756.

Veeraraghavan R, Salama ME, Poelzing S (2012). Interstitial volume modulates the conduction velocity-gap junction relationship. Am J Physiol Heart Circ Physiol 302, H278–H286.

Vite A, Radice GL (2014). N-cadherin/catenin complex as a master regulator of intercalated disc function. Cell Commun Adhes 21, 169–179.

Weibrecht I, Leuchowius KJ, Clausson CM, Conze T, Jarvius M, Howell WM, Kamali-Moghaddam M, Soderberg O (2010). Proximity ligation assays: a recent addition to the proteomics toolbox. Expert Rev Proteomics 7, 401–409.

Zinchuk V, Grossenbacher-Zinchuk O (2014). Quantitative colocalization analysis of fluorescence microscopy images. Curr Protoc Cell Biol 62, Unit 4.19.